International Journal of Applied Earth Observation and Geoinformation 38 (2015) 204–215

Contents lists available at ScienceDirect

International Journal of Applied Earth Observation and Geoinformation

journal homepage: www.elsevier.com/locate/jag

# Using remote sensing to monitor the influence of river discharge on watershed outlets and adjacent coral Reefs: Magdalena River and Rosario Islands, Colombia

Max J. Moreno-Madriñán [a,*], Douglas L. Rickman [b], Igor Ogashawara [c], Daniel E. Irwin [d], Jun Ye [e], Mohammad Z. Al-Hamdan [f]

[a] Department of Environmental Health, Fairbanks School of Public Health at Indiana University, IUPUI, Indianapolis, IN 46202, USA
[b] Global Hydrology and Climate Center, Earth Science Office at NASA Marshall Space Flight Center, Huntsville, AL 35805, USA
[c] Department of Earth Science, School of Science at Indiana University-Purdue University, IUPUI, Indianapolis, IN 46202, USA
[d] SERVIR, Earth Science Office at NASA Marshall Space Flight Center, Huntsville, AL 35805, USA
[e] Department of Statistics at The University of Akron, Akron, OH 44325, USA
[f] Science and Technology Institute, Universities Space Research Association at NASA Marshall Space Flight Center, Huntsville, AL 35805, USA

ARTICLE INFO

*Article history:*
Received 27 September 2014
Received in revised form 10 January 2015
Accepted 16 January 2015
Available online 30 January 2015

*Keywords:*
Remote sensing
MODIS
TRMM
Water quality
Suspended sediments

ABSTRACT

Worldwide, coral reef ecosystems are being increasingly threatened by sediments loads from river discharges, which in turn are influenced by changing rainfall patterns due to climate change and by growing human activity in their watersheds. In this case study, we explored the applicability of using remote sensing (RS) technology to estimate and monitor the relationship between water quality at the coral reefs around the Rosario Islands, in the Caribbean Sea, and the rainfall patterns in the Magdalena River watershed. From the Moderate Resolution Imaging Spectroradiometer (MODIS), this study used the water surface reflectance product (MOD09GQ) to estimate water surface reflectance as a proxy for sediment concentration and the land cover product (MCD12Q1 V51) to characterize land cover of the watershed. Rainfall was estimated by using the 3B43 V7 product from the Tropical Rainforest Measuring Mission (TRMM). For the first trimester of each year, we investigated the inter-annual temporal variation in water surface reflectance at the Rosario Islands and at the three main mouths of the Magdalena River watershed. No increasing or decreasing trends of water surface reflectance were detected for any of the sites for the study period 2001–2014 ($p > 0.05$) but significant correlations were detected among the trends of each site at the watershed mouths ($r = 0.57$–$0.90$, $p < 0.05$) and between them and the inter-annual variation in rainfall on the watershed ($r = 0.63$–$0.67$, $p < 0.05$). Those trimesters with above-normal water surface reflectance at the mouths and above-normal rainfall at the watershed coincided with La Niña conditions while the opposite was the case during El Niño conditions. Although, a preliminary analysis of inter-annual land cover trends found only cropland cover in the watershed to be significantly correlated with water surface reflectance at two of the watershed mouths ($r = 0.58$ and $0.63$, $p < 0.05$), the validation analysis draw only a 40.7% of accuracy in this land cover classification. This requires further analysis to confirm the impact of the cropland on the water quality at the watershed outlets. Spatial analysis with MOD09GQ imagery detected the overpass of river plumes from Barbacoas Bay over the Rosario Islands waters.



## 1. Introduction

Water turbidity and associated light attenuation, resulting from excessive sediment deposition rates are factors widely known to limit coral reef development. The effects of terrigenous sediments have been suggested to be among the main factors leading to the deterioration of coral reefs in a 145 km$^2$ complex of coral continental shelf reef located around the Rosario Islands (Díaz et al., 2000; Cendales et al., 2002), in the southeastern Caribbean Sea offshore 30 km from Cartagena, Colombia (Figs. 1 and 2). Runoff and maximum water discharge have been identified as the main physical determinants of sediment yield from the Magdalena River near the

* Corresponding author. Tel.: +1 8135059305/317 274 3170.
*E-mail address:* mmorenom@iu.edu (M.J. Moreno-Madriñán).

http://dx.doi.org/10.1016/j.jag.2015.01.008

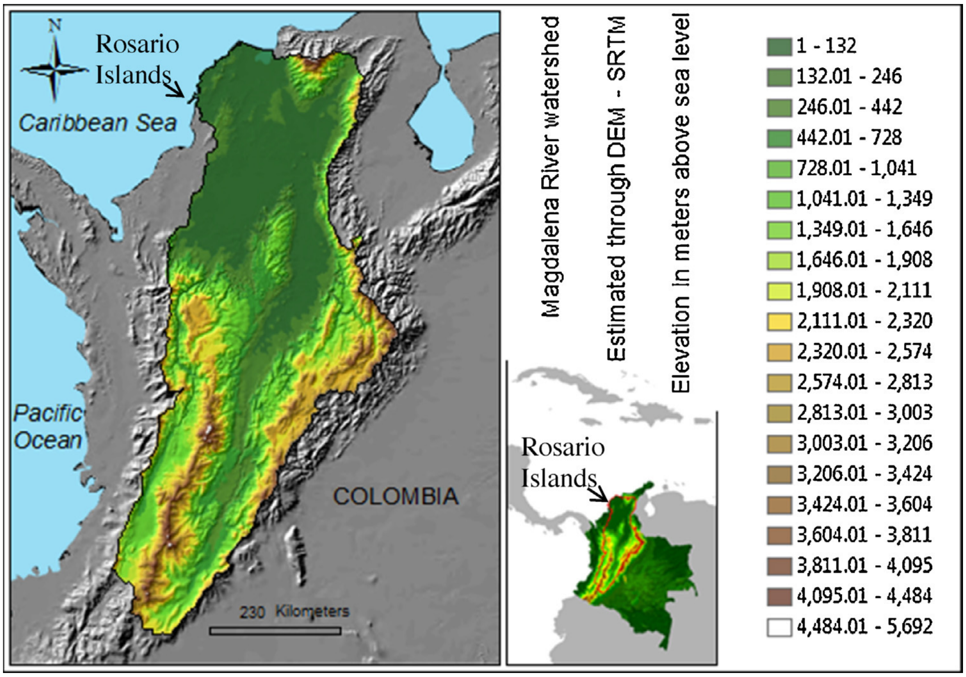


**Fig. 1.** Location of Rosario Islands at the outputs of the Magdalena River and location of the Magdalena River Basin in Colombia and South America.

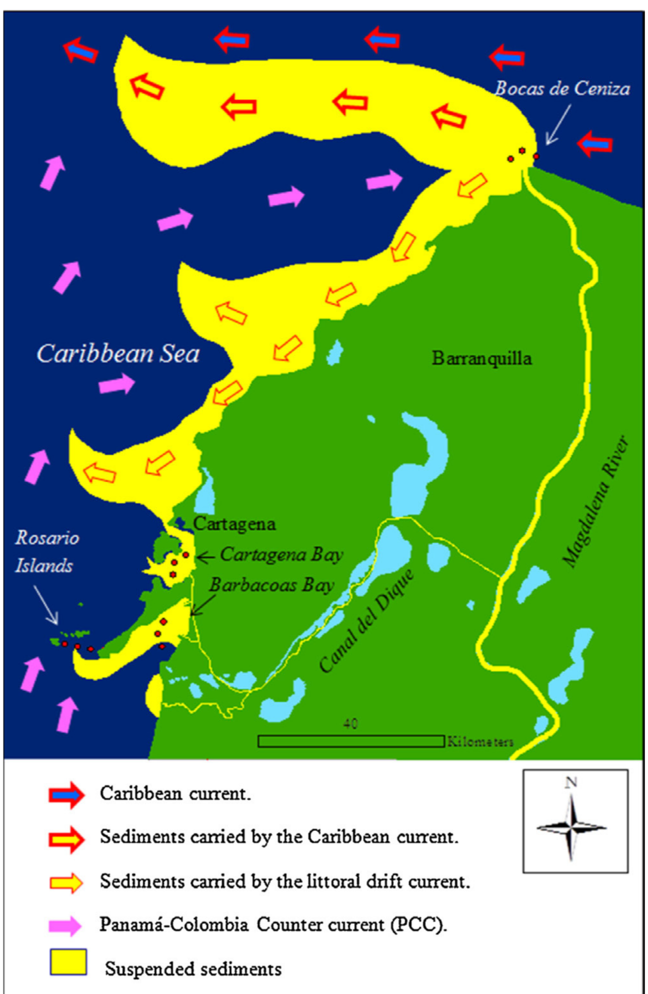


**Fig. 2.** Site locations and dispersion of the Magdalena River sediments in the Sea.

islands (Restrepo et al., 2006a). Regarding, cultural determinants, it has been proposed that continuous dredging and enlargement in a channel that divert waters from the Magdalena River along with the increasing human activities on the river watershed are among the main factors negatively affecting the coral reef of the Rosario Islands (Restrepo et al., 2006b; Mogollón-Vélez, 2013). It is clear that identifying the main stressors on the islands' corals is critical to effectively make corrections and plan ahead for proper sustainable management. Easily accessible cost efficient methods that facilitate long term ongoing analysis can be of high value. Such methods need to be proven for their sensitivity to identify potential spatial and temporal trends in the discharges and distribution of sediments likely to influence the coral reefs at the Rosario Islands. Knowledge of these trends will facilitate further studies to explore relationships with human activities in the watershed and mechanisms to correct or ameliorate negative effects.

A major difficulty to performing temporal trends investigations is the lack of historical *in situ* data as these are labor intensive, expensive and require investing long periods of time to accumulate enough data for analysis. Alternatively, remote sensing (RS) technology offers the advantage of archives for retrospective studies, with freely available data from places not monitored *in situ*, which could draw useful results in the short and long term. Surface reflectance MODIS (Moderate Resolution Imaging Spectroradiometer) 250 m product at 620–670 nm has been well established to estimate suspended sediments and turbidity in estuarine waters (Hu et al., 2004; Chen et al., 2007; Rodríguez-Guzmán and Gilbes-Santaella, 2009; Petus et al., 2010; Moreno Madriñan et al., 2010; Doxaran et al., 2009; Miller et al., 2011). The red section of the electromagnetic spectrum is commonly used in coastal waters to estimate sediments/turbidity because most of the reflectance spectra at this wavelength are dominated by suspended sediments rather than by pure water or other water constituents like phytoplankton and Colored Dissolved Organic Carbon (CDOM) (Mobley, 1994). We are unaware of any data on turbidity or total suspended matter concentration in our study sites for the time period of analysis. Given the scarcity of historical *in situ* data for the selected sites, this study was an effort to assess whether satellite data alone could be used to identify temporal and spatial patterns in water surface reflectance, as surrogate for sediments loadings, at spatial points where discharges from the Magdalena River watershed are possibly influencing the coral reefs at the Rosario Islands. Temporal rainfall patterns in the watershed were explored for possible effects on water surface reflectance. Complementarily, preliminary analysis explored for a possible relationship between such water surface reflectance and land cover in the watershed.

## 2. Spatial and historical background

The archipelago of the Rosario Islands, which has been a natural Park since 1978 (Díaz et al., 2000), lies in the Intertropical Convergence Zone (Sánchez et al., 1999) with mean annual seawater temperature, rainfall, and salinity of 27.5 °C, 1013.1 mm, and 35‰, respectively (Sánchez, 1995). In general, the scarcity of coral reefs near river mouths can be easily explained by the high turbidity and rate of sedimentation in these areas (Ferre-D'Amaré, 1985, as cited in Carricat-Ganivet and Merino, 2001; Cortés and Risk, 1985). The existence of the coral reef formation of the Rosario Islands near the mouths of the Magdalena River is due to the fact that the discharges through Bocas de Ceniza, do not reach this coralline formation (Mogollón-Vélez, 2013) since they are carried west-northwestward by the Caribbean Current (Wust, 1963; Morrison and Nowlin, 1982) and not southward. Although a portion of these suspended sediments is transported toward the south-west along the coast by the littoral drift current yet they are encountered by the clear waters of the Panama-Colombia Counter current (PCC), which flows northeastward along the Caribbean cost of Colombia (Pujos et al., 1986) (Fig. 2) and the resulting sediment plume is also diluted northwestward before reaching the islands at the south-west as it can be confirmed by MOD09GQ images on Figs. 5 and 6. Direct discharges from the Canal del Dique into the bays of Barbacoas and Cartagena, which are much closer to the influence zone of the Rosario Islands, did not start before 1952 (Mogollón-Vélez, 2013). The Canal del Dique was further enlarged and rectified in 1984 with a resulting considerable increase in sediment loads (Mogollón-Vélez, 2013). The water discharge through the Canal del Dique has been calculated in about 397 $m^3\,s^{-1}$ (Restrepo et al., 2006b), of which approximately 35% is discharged into Barbacoas Bay through two outlet channels (Matunilla and Lequerica), 17.5% is discharged through an outlet channel further south of this bay, which is called Correa. Other 34% is discharged in Cartagena Bay and the approximately remaining 15.5% is received by wetlands along the Canal or is lost to evaporation (Mogollón-Vélez, 1913). Due to this location relative to the PCC and Rosario Islands, the discharge into Barbacoas Bay and that through the Correa outlet channel are of particular concern.

Human population within river watersheds is directly associated with sediments loading at the mouths of the rivers (West and Woesik, 2001). Located in the Andean region of Colombia, SA (Fig. 1) and with a population density of 120 inhabitants $km^{-2}$, the Magdalena River watershed, houses the eighty percent of the Colombian population (Restrepo and Kerfve, 2004). An annual rainfall of about 2050 mm $yr^{-1}$ across the entire watershed is drained throughout an area of approximately 257,438 $km^2$ (~24% of the country territory and the largest watershed of any Andean river) (IDEAM, 2001) discharging a mean annual of about 7200 $m^3\,s^{-1}$ into the southwestern Caribbean (Restrepo et al., 2001b). These discharges range between mean annuals of 5512 $m^3\,s^{-1}$ and 8747 $m^3\,s^{-1}$, during El Niño and La Niña years respectively (Restrepo et al., 2006b). The watershed highest elevations surpass the 5000 m above mean sea level (Fig. 1), its general relief has pronounced slopes frequently steeper than 35° with increasing changes in land cover/land use, which yield 560 t $km^{-2}\,yr^{-1}$ of sediments (Restrepo et al., 2006b), the river has the largest sediment yield from any South American river in the Atlantic Ocean (Restrepo and Kjerfve, 2004) and the greater sediments fluxes on the Caribbean Sea (Restrepo and Kjerfve, 2002).

**Table 1**
Geo-location of sites used for water surface reflectance monitoring.

| Site | Sub-site | Latitude | Longitude |
|---|---|---|---|
| Bocas de Ceniza | A | 11.0117 | −74.879 |
| | B | 11.134 | −74.857 |
| | C | 11.123 | −74.829 |
| Cartagena Bay | A | 10.294 | −75.555 |
| | B | 10.319 | −75.551 |
| | C | 10.334 | −75.528 |
| Barbacoas Bay | A | 10.153 | −75.576 |
| | B | 10.176 | −75.586 |
| | C | 10.201 | −75.573 |
| Rosario Islands | A | 10.157 | −75.770 |
| | B | 10.152 | −75.744 |
| | C | 10.147 | −75.718 |

## 3. Materials and methods

This analysis was approached in two sections, one analyzing the water surface reflectance at the watershed outlets and adjacent coral reefs at the Rosario Islands and other exploring the watershed as possible source of influencing factors. For the first section, GoogleEarth™ was used to locate three sub-sites at the mouth of the main outlet (Matunilla) discharging from the Canal del Dique into Barbacoas Bay and these three sub-sites were considered a site. The sub-sites were distributed spatially forming a semi arc around the mouth of the channel, and they are ~3000 m apart and at ~3000 m from the mouth as seen in Fig. 2 (sites' geographic coordinates are given in Table 1). For comparison purposes, a same criterion was followed to choose sites on the mouth from the Canal del Dique into Cartagena Bay and on that from the Magdalena River into the Caribbean Sea at Bocas de Ceniza (Fig. 2). For further comparison with low sediments waters, a fourth site composed of three 3000 m-apart sub-sites was arranged along an imaginary straight line between the most western point of the Barú Island and the most eastern point of the Rosario Island (one of the Rosario Islands archipelago) (Fig. 2 and Table 1). Such methodology resulted in a total of 12 sub-sites. GoogleEarth™ was also used in the watershed analysis to generate control points for the validation of a preliminary classification of MODIS land cover. The methods deployed to undertake each section of the analysis are described below by section along with a description of data products used.

### 3.1. Water surface reflectance analysis

Thirteen years (2001–2013) of MODIS/Terra Surface Reflectance Daily L2G Global 250 m SIN Grid V005 (MOD09GQ) were downloaded from the EOS Clearing House (ECHO) website of NASA's Earth Observing System Data and Information System (EOSDIS, 2013). MOD09GQ is geolocated and estimates the reflectance at sea level without atmospheric absorption and scattering effect. A detailed process of the atmospheric correction for this product is described by Doxaran et al. (2009). Surface reflectance data is provided in two channels, one in the visible range between 620 and 670 nm (Band 1) and one in the near-infrared between 841 and 876 nm (Band 2). The visible range was used in this study. MODIS 250 m surface reflectance is a land product, however, the tiles covering coastal lands include also the adjacent coastal waters. Compared with ocean waters, the higher concentration of suspended sediments in coastal and inland waters results in higher surface reflectance, which has been capitalized by several researchers studying suspended sediments in estuarine and inland waters (Hu et al., 2004; Chen et al., 2007; Rodríguez-Guzmán and Gilbes-Santaella, 2009; Petus et al., 2010; Moreno Madriñán et al., 2010; Doxaran et al., 2009; Miller et al., 2011). QC layers accompanying this product need to be used with extra care since it was not designed for water reflectance therefore there is no validation that water pixels are accurate. Consequently, all daily images downloaded for the study period were visually inspected individually for cloud cover and black pixels containing negatives values.

As a QC procedure, images having more than one pixel covering a sub-site with any of the following two criteria were excluded from the analysis: (1) being covered by cloud or fog; or (2) intercepted by black pixels (which draw a negative value as surface reflectance). This procedure resulted in few images available during the periods from April to middle of June (91–166 Julian days) and from around the first quarter of August through November (220–334 Julian days) (Fig. 3), which roughly coincided with the two annual rainy periods in the study area (Restrepo et al., 2006a). Availability of good quality images during the rainy period varied from year to year. Consequently, most suitable images were available for the period December–March (longer dry period) and specially January–March (0–90 Julian days) (consistently for all the studied years) (Fig. 3). In this study, only images from the latter interval (the first quarter of the year, 0–90 Julian days) were used throughout the 2001–2014 study period in order to have consistency of good quality images. 2001 was the first year with a complete yearlong data from Terra satellite.

The “extract values to point” function of ArcGIS 10.2 was used to extract the water surface reflectance at each of the sub-sites, from the selected images. For each site, a mean daily value of water surface reflectance was calculated from its three sub-sites for each image. Median water surface reflectance was calculated for each site for the first quarter of the year (0–90 Julian days) from the selected images. The three months median as opposed to the arithmetic mean was used in order to counteract the variability in the daily data. After applying exclusion criteria, the numbers of daily images used to obtain each three months median value were: 12, 11, 10, 19, 12, 14, 14, 19, 14, 11, 18, 14, 12 and 16 for years 2001–2014, respectively. The three months medians per site, calculated as described, were plotted into an inter-annual time series along the 2001–2014 time period (Fig. 4a) and trend lines were analyzed for significance using the proc mixed method in SAS statistical software version 9.4. These trend lines of water surface reflectance per site are assumed to provide an approximation of the inter-annual temporal trends of suspended sediments in the water during the study period, for the four sites: Bocas de Ceniza, Cartagena Bay Barbacoas Bay and Rosario Islands.

### 3.2. Analysis of watershed processes

Digital Elevation Model (DEM) data from the Shuttle Radar Topography Mission (SRTM) was downloaded from the Global Data Explorer website of the Land Processes Distributed Active Archive Center (LP DAAC, 2013) within the NASA EOSDIS. These data were processed with ArcMap 10.2 and used to delineate the Magdalena River watershed for analysis of relationships between processes at the watershed and its outlets. The delineated watershed subset was used to extract a gridded dataset of monthly precipitation from the Tropical Rainfall Measuring Mission (TRMM), using the “extract by mask” function of ArcGIS 10.2. An estimate of inter-annual rainfall temporal trend throughout the watershed was calculated to test the expected relationship with temporal trends of water surface reflectance at the outlets. These data were accumulated for the three months periods corresponding to the selected water surface reflectance data and likewise plotted into an inter-annual time series for the period 2001–2014 and under-laid with the plotted water surface reflectance (Fig. 4a). Trend line significance was analyzed with SAS 9.4 proc mixed method while SAS 9.4 proc corr method with Spearman correlation ($r$) was used to explore relationships between estimated rainfall trends and water surface reflectance trends. Complementarily, same procedure was followed to analyze for significance of inter-annual trend line using annual rainfall for the period 2001–2013. Data of monthly precipitation from the $0.25^\circ \times 0.25^\circ$ TRMM product 3B43 V7 were downloaded from the TRMM Online Visualization and Analysis System (TOVAS) at the Goddard Earth Sciences Data and Information Services Center (GES DISC, 2014). TRMM is a joint mission between NASA and the Japan’s National Space Development Agency.

Although MODIS Land Cover product, MCD12Q1 V51 type 1, is designed for land use characterization and not specifically to study land cover change (Friedl et al., 2010), it was useful in our study to preliminarily suggest the possible contributing influence of land cover classes in the behavior of water surface reflectance. This yearly product combines data from MODIS sensors on board Terra and Aqua satellites and provides a characterization of land cover using 16 land classes in 463 m of spatial resolution. Related land classes were grouped together in broader classes since some of the specific classifications were not applicable to the tropical ecology of the study area and generally to simplify the land use characterization process. Consequently, the five specific land classes related to forest were aggregated into one called forest. Two classes related to shrublands became one called shrubland. Three classes including either savannas or grasslands became a broader one called savanna. Likewise, a broad cropland class in this study encompasses two specific croplands classes of the original product classification. The remaining five land classes remained the same as in the original classification though with simpler names as follow: water, wetland, urban, snow and barren. This approach resulted in nine land classes overall.

Complete information about the product and its 16 original land classes is available at the US Geological Survey (USGS)/Land Processes Distributed Active Archive Center (LP DAAC, 2014). The analysis of land cover characterization was conducted for the time period 2001–2012, since this annual product was not yet available for 2013 on. Data were downloaded from the Reverb ECHO website (2013). As with the products already described, land cover data were extracted to the watershed subset with the “extract by mask” function of ArcGIS 10.2. Annual land cover classes were plotted for the time period 2001–2012 and analyzed for temporal trend significance using statistical software SAS 9.4 proc mixed method. Subsequently, such trends were analyzed for correlation with water surface reflectance trends at the watershed outlets using SAS 9.4 proc corr method. Land cover validation was evaluated using a confusion matrix made by 20 control points per each of the following land classes: cropland, grassland, forest, urban, water and wetland. These points were collected by personal knowledge of the area and using high spatial resolution images on Google Earth to identify the coordinates.

## 4. Results

### 4.1. Data distribution

Scatter plots between the water surface reflectance data (that passed QC exclusion criteria) and Julian days per year for all four sites during the period 2001–2003 is displayed in Fig. 3. As expected from the low cloud coverage during the annual dry season, it is clear from Fig. 3 that the annual plots of available water surface reflectance data were concentrated in this longer dry period in the

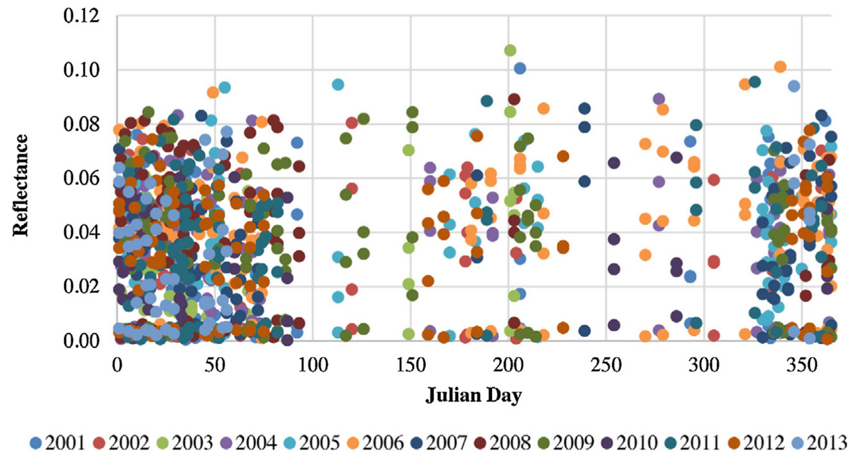


**Fig. 3.** Scatter plots between days of free cloud reflectance measurements during the year and the reflectance measurements at the four monitoring sites: Bocas de Ceniza, Cartagena Bay, Barbacoas Bay and Rosario Islands.

region, December–March, and especially during January–March (0–90 Julian days). A slight concentration of data was available during Julian days 166 and 220, which roughly corresponds to the shorter dry season (166–196 Julian days). This shorter dry period at the middle of the year is known by the local terminology as the "Veranillo de San Juan" (Saint John's little summer). Similar concentration pattern toward the dry periods according to the bimodal rainfall regimen on the Magdalena River watershed (Restrepo et al., 2006a) was detected at each one of the four sites. Although there is a MODIS 8-day composite product for surface reflectance (MOD09Q1), which reports data only for clear sky pixels, thus probably allowing data covering all year around, such was not used since different sites would have resulted with surface reflectance values from different number of pixels. This would have not allowed a consistent treatment for each one of the sites needed to compare trends evenly.

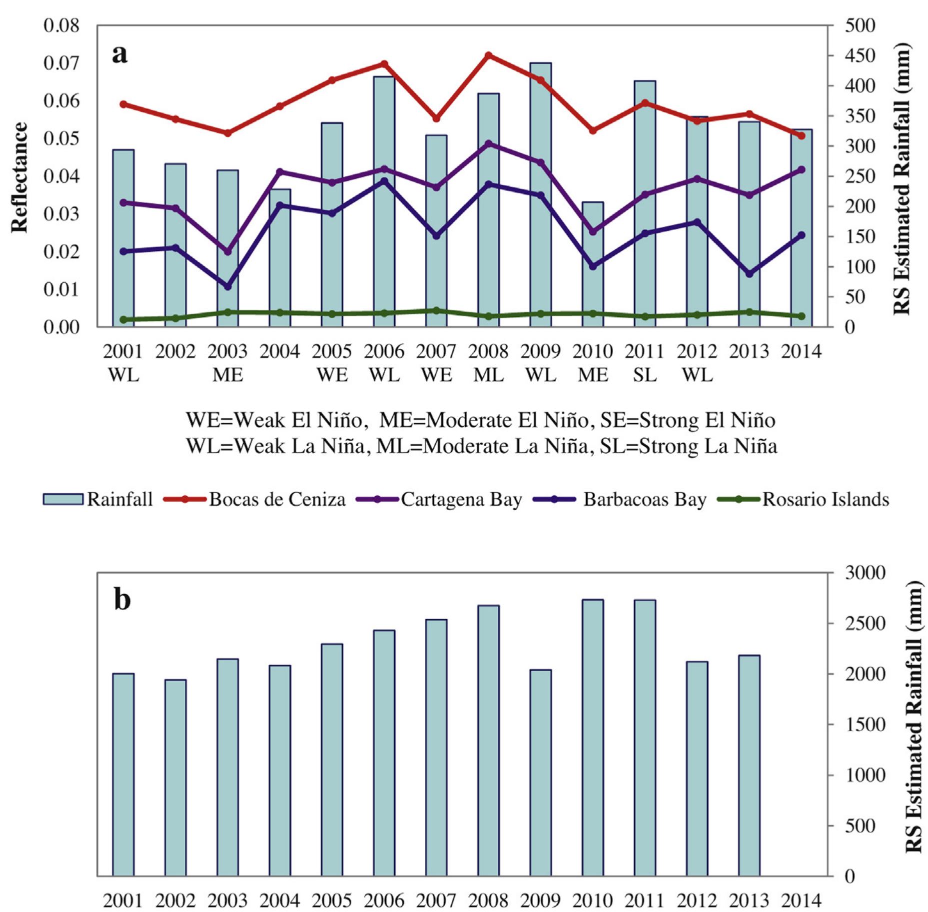


**Fig. 4.** In lines, time series of inter-annual mean cloud free median surface reflectance (MOD09GQ) during the first 90 days of each year for the four sites monitored. In bars, time series of accumulated TRMM estimated rainfall at the Magdalena River basin during the first 90 days of the year for the period 2001–2014 (a) and the entire year for the period 2001–2013 (b).

### 4.2. Temporal trends and its correlations

For water surface reflectance at each of the four study sites, the 2001–2014 inter-annual temporal trends (histogram) depicted in Fig. 4a were not significantly increasing or decreasing ($p > 0.05$). Similarly, no significance was detected in the 2001–2014 inter-annual temporal trend of the rainfall precipitated on the Magdalena River watershed, when considering solely the three first months of each year (Fig. 4a). However, a significant inter-annual temporal trend was noticed when considering the rainfall along the entire year and for the period 2001–2013, the inter-annual temporal trend was found to be significant (Histogram of Fig. 4b, $p < 0.01$).

When using the first three months of rainfall per year, moderate positive correlation were found between the 2001–2014 inter-annual temporal trend of rainfall at the Magdalena River watershed and the corresponding trends for water surface reflectance at the three watershed outlet study sites (Bocas de Ceniza, Cartagena Bay and Barbacoas Bay Table 2). These correlations were significant ($p < 0.05$ or 0.01). Yet such significant correlation between trends of rainfall on the watershed and water surface reflectance was not detected when considering the Rosario Islands site ($p > 0.05$, Table 2). Likewise, the water surface reflectance trend line at the Rosario Islands site was weakly correlated with each of the water surface reflectance trends at the three outlet study sites (Table 2) and the correlations were not significant ($p > 0.05$). The water surface reflectance trend line at Barbacoas Bay site was strongly correlated with those of Cartagena Bay and Bocas de Ceniza but the latter two were just moderately correlated between each other (Table 2). All three outlet study sites were significantly correlated among themselves ($p < 0.05$ or 0.01).

### 4.3. El Niño/La Niña

The fluctuation in the 2001–2014 inter-annual trend of water surface reflectance at the Bocas de Ceniza site (the main outlet of the Magdalena River watershed) fitted the sequence of El Niño/La Niña years (Fig. 4a). The first three months of each studied year were named El Niño, La Niña or none according to the classification of the Oceanic Niño Index (ONI) threshold of +/−0.5 °C (CPC, 2014). Based on this, warm trimesters were considered El Niño episodes while La Niña episodes corresponded to cold trimesters. Those trimesters not exceeding the ONI threshold were neither El Niño nor La Niña. Those years when the first three months were described as El Niño episodes, coincided with depressions in the reflectance trend while the peaks in such trend tended to coincide with years when the first three months concurred with La Niña episodes. This coincidence of reflectance depression/El Niño and reflectance peak/La Niña was also observed for the two outlets study sites of the Canal del Dique (Cartagena Bay and Barbacoas Bay) up to year 2011. During years 2012–2014, these two sites continued presenting fluctuations in reflectance trends parallel with each other (as it was the case during the entire study period) but different as compared with that at Bocas de Ceniza. No pattern was detected between the inter-annual water surface reflectance trend at the Rosario Islands site and the fluctuations of El Niño/La Niña years. By the most part, the trend in RS estimated rainfall fitted as expected the sequence of El Niño/La Niña, tending to coincide the years with lower RS estimated rainfall with El Niño years while La Niña years with those having higher rainfall (Fig. 4).

### 4.4. Turbidity plumes

A visual inspection of MOD09GQ imagery (Fig. 5a–l) clearly supports an agreement between the water surface reflectance and the description found in literature (Restrepo and Lopez, 2007; Libhaber, 2004) (graphically depicted on Fig. 2) about the discharge

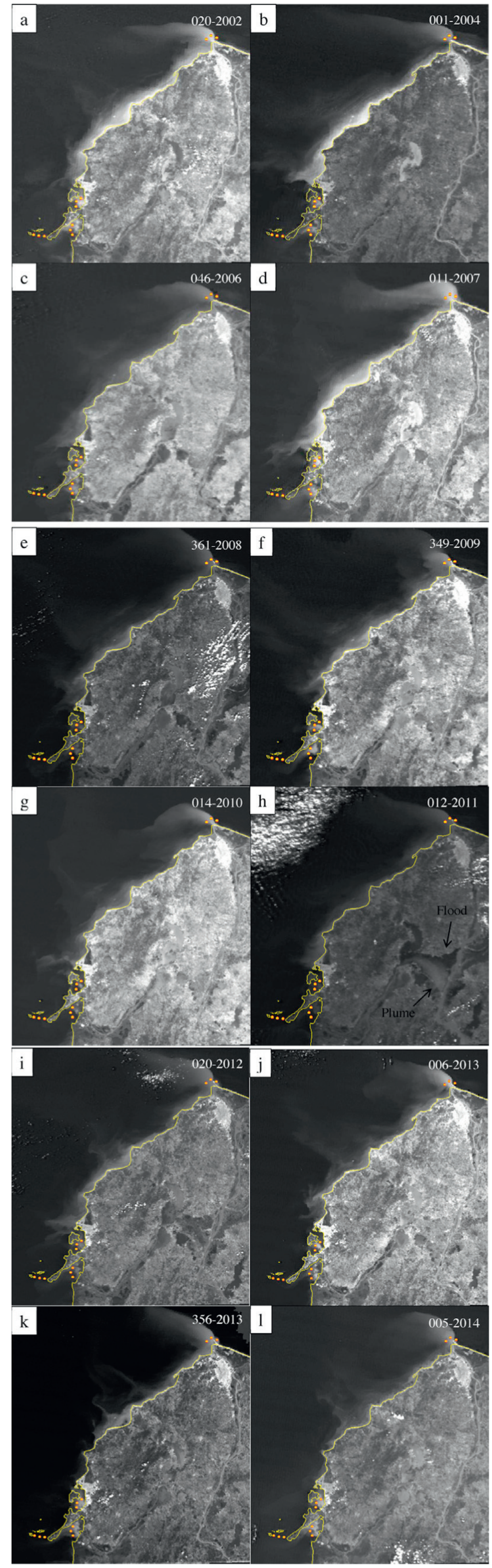


**Fig. 5.** MOD09GQ (Band 1) images of the Magdalena River floodplain showing the sites locations at the outputs of the Magdalena River watershed. (a) January 20, 2002; (b) January 1, 2002; (c) February 15, 2006; (d) January 11, 2007; (e) December 26, 2008; (f) December 15, 2009; (g) January 14, 2010; and (h) January 12, 2011.

**Table 2**
Spearman correlations between temporal trend lines of MOD09GQ surface reflectance at the four sites analyzed and annual rainfall in the Magdalena River watershed. Correlations were calculated with SAS: proc corr method, * = $r$ with $p < 0.05$, ** = $r$ with $p < 0.01$.

| | | Surface reflectance trend lines | | | | Rainfall |
|---|---|---|---|---|---|---|
| | Spearman correlations | Rosario Islands | Bocas de Ceniza | Cartagena Bay | Barbacoas Bay | Trend line |
| Surface reflectance trend lines | Rosario Islands | 1 | | | | |
| | Bocas de Ceniza | −0.17 | 1 | | | |
| | Cartagena Bay | −0.08 | 0.57* | 1 | | |
| | Barbacoas Bay | −0.16 | 0.71** | 0.90* | 1 | |
| Precipitation rainfall trend line | | −0.16 | 0.64** | 0.67* | 0.63* | 1 |

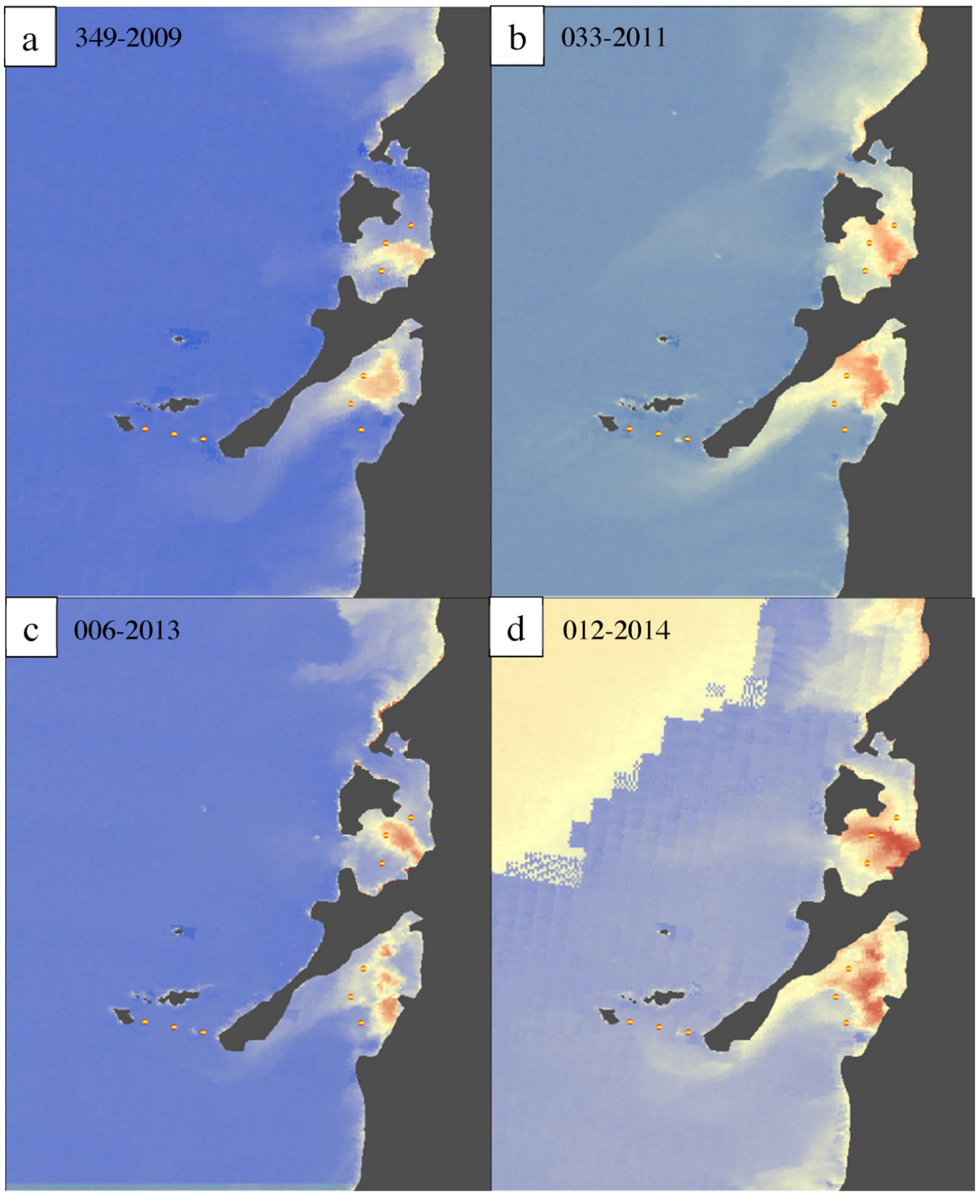


**Fig. 6.** MOD09GQ (Band 1) images showing plumes of sediments from the Canal del Diqueinto Cartagena Bay (Top) and Barbacoas Bay (Bottom). Notice the sediment plume in Barbacoas Bay bordering Barú and heading north toward the Rosario Islands. (a) December 15, 2009, (b) February 2, 2011, (c) January 6, 2013 and (d) January 12, 2014.

and transport of suspended sediments in the study area waters. A plume of high water surface reflectance advances from Bocas de Ceniza south-westward along the cost (Restrepo and Lopez, 2007) to encounter the PCC from the south-west (Pujos et al., 1986) in the proximity of Cartagena City to be then dispersed into the Caribbean Sea. This dispersion or dilution occurs north of the Rosario Islands thus being unlikely that the Bocas de Ceniza plume would importantly affect the coral reefs in the islands. A zoom into de bays of Cartagena and Barbacoas (Fig. 6a–d) suggests that the plume from Cartagena Bay might at most slightly influence the northernmost of the Rosario Islands. A different depiction appears to be the case for the plume coming from Barbacoas Bay. This plume comes from the south. After bordering the peninsula-like island of Barú this plume is transported north by the PCC across the Rosario Islands having the most likely impact on the Islands's coral reefs among all the plumes from the Magdalena River.

### 4.5. Preliminary land cover analysis

Other important factor influencing the sediments loads in the watersheds outlets, thus in the water surface reflectance, is the human activity taking place on the watershed (Fabricius et al., 2012). This has been mentioned in the literature to be increasing (Díaz et al., 2000; Restrepo et al., 2006b). A preliminary characterization of the Magdalena River Watershed using MODIS Land Cover product, MCD12Q1 V51 type 1, is shown in Table 3. As explained in the methods, some land classes have been re-grouped as several of the classes from this product do not apply in our study. The land characterized as forest by this product include large portions of weeded land and other various types of land that although not properly forest do not meet the criteria of the other land classes either. With a 26.9% of the total watershed in 2012 (most recent year released by this product) lands characterized with some type of cropland activity composed one of the three most extent land class after forest and weeds 41.6% followed by grasslands and pastures 25.5% (Table 3). Fig. 7 displays a characterization of land cover in (a) 2001 and (b) 2012, most recent year of this product release. Fig. 8). Such association was significant with Bocas de Ceniza and Barabacoas Bay ($p < 0.05$) and marginally significant with Cartagena Bay ($p = 0.054$). Table 5 depicts a time series of the 2001–2012 inter-annual trends of land cover where the land covered with forest and other weeded and high vegetation presented a significant increase ($p < 0.01$) while grasslands and pastures a significant decreasing trend ($p < 0.01$). Croplands increased from 2001 to 2006 and decreased from 2007 to 2012

**Table 3**
Percentages of land cover composition of the total Magdalena River watershed area in 2012 and summary of trend line analysis for the period 2001–2012. Analysis of trend lines was conducted with SAS, proc mixed method.

| Analysis of land cover | | Analysis of tend significance | |
|---|---|---|---|
| Land class | Percent of the total | Estimate | $p$ |
| Forest | 41.57 | 1432.9 | <0.0001 |
| Grassland | 25.50 | −2600.18 | <0.0001 |
| Cropland | 26.94 | 609.29 | 0.075 |
| Wetland | 2.83 | 442.57 | 0.19 |
| Water | 1.59 | 245.14 | 0.47 |
| Urban | 1.06 | −1.238 | 1.00 |
| Shrubland | 0.47 | −104.54 | 0.75 |
| Barren | 0.03 | −21.18 | 0.95 |
| Snow | 0.02 | 4.99 | 0.99 |

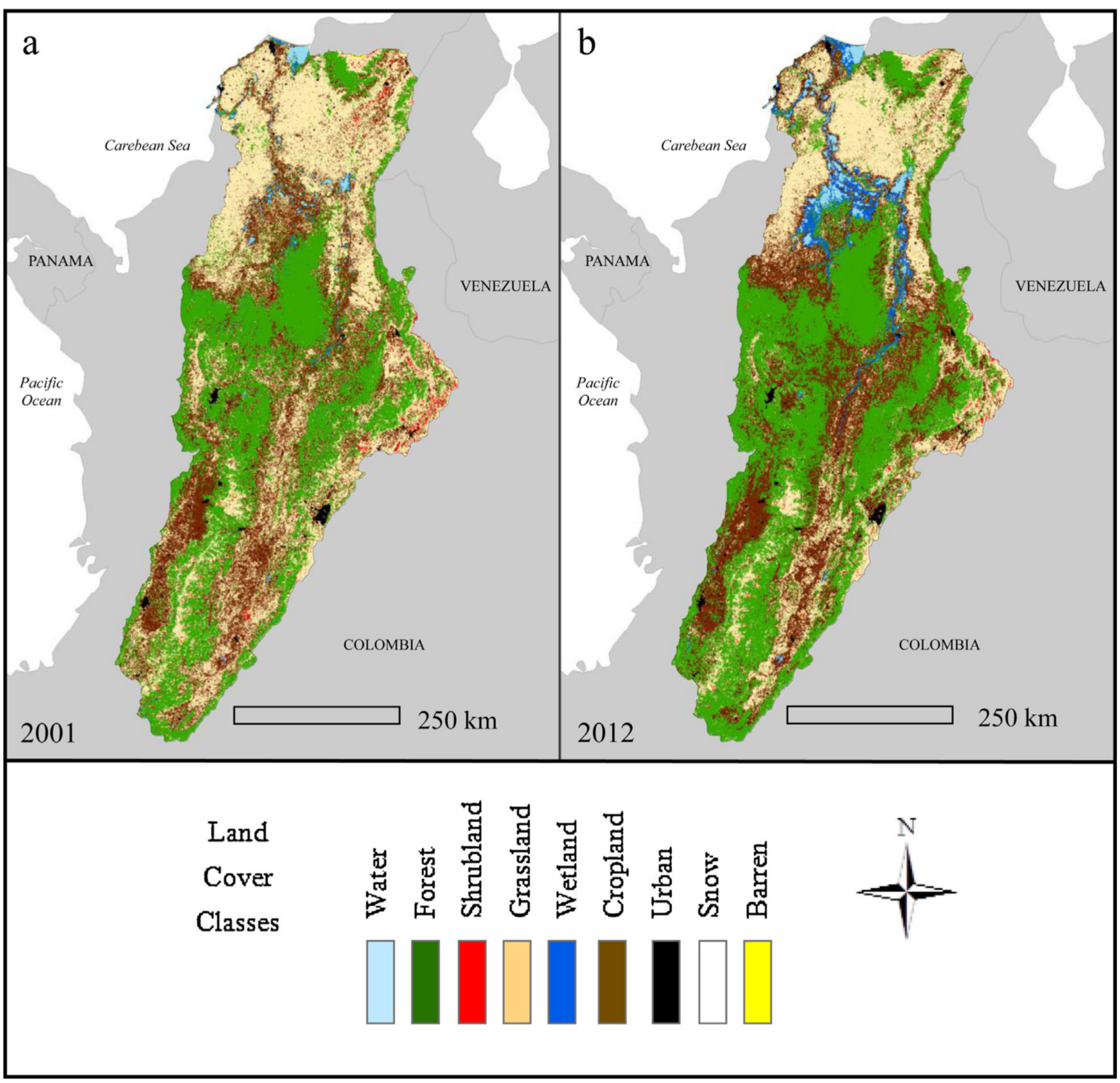


**Fig. 7.** Annual composites of land cover in the Magdalena River basin for years (a) 2001 and (b) 2012 for the nine land classes used in this study. These land classes were derived and adjusted from MODIS Land Cover product, MCD12Q1. Although there is a significant increase in water and wetland cover when considering each class independently, this increase is not significant when considered relative to the entire watershed. Such increase may be due to the high rainfall associated to the La Niña years from the second half of 2010 to the first half of 2012.

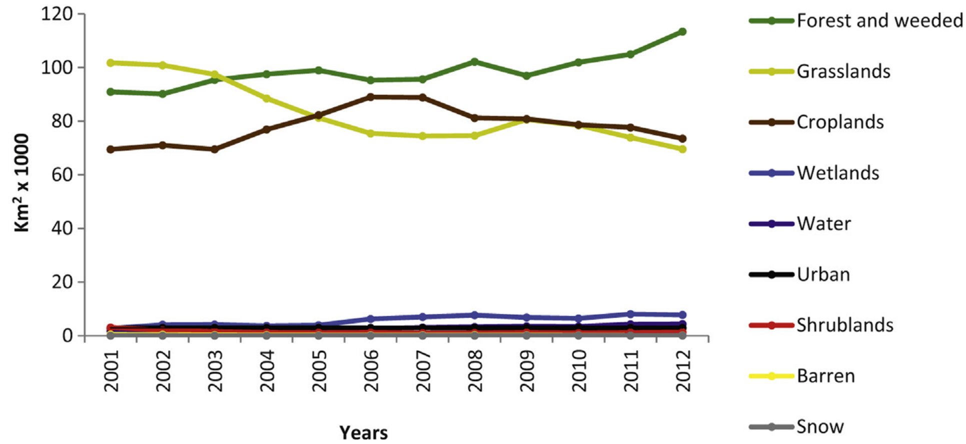


**Fig. 8.** Times series of inter-annual change of the nine land cover classes adjusted from MODIS Land Cover product, MCD12Q1, for the time period 2001–2012.

**Table 4**
Summary of Spearman correlation ($r$) analysis between the MODIS estimated inter-annual trends of land cover change in the Magdalena River watershed and those of MODIS estimated annual median surface reflectance at the four sites (three river outlets and Rosario Islands). This table only includes major land cover classes. All other land classes together encompassed less than 6 percent of the total watershed and presented no significant correlation ($r$) with site trends at the watershed outlets ($p > 0.05$). * = $r$ with $p < 0.05$, ** = $r$ with $p < 0.01$.

| Land cover class | Bocas de Ceniza | Cartagena Bay | Barbacoas Bay | Rosario Islands |
|---|---|---|---|---|
| Forest and weeded | 0.07 | 0.29 | 0.23 | 0.90 |
| Grassland and Savannahs | −0.16 | −0.39 | −0.36 | −0.14 |
| Cropland | 0.58* | 0.56 | 0.63* | 0.40 |

**Table 5**
Confusion matrix for the MCD12Q1 product on the Magdalena River watershed.

| | Cropland | Grassland | Forest | Urban | Water | Wetland | |
|---|---|---|---|---|---|---|---|
| Cropland | 11 | 7 | 2 | 0 | 0 | 0 | 20 |
| Grassland | 6 | 12 | 1 | 0 | 0 | 1 | 20 |
| Forest | 4 | 4 | 12 | 0 | 0 | 0 | 20 |
| Urban | 1 | 0 | 1 | 18 | 0 | 0 | 20 |
| Water | 0 | 0 | 0 | 0 | 17 | 3 | 20 |
| Wetland | 5 | 0 | 2 | 0 | 2 | 11 | 20 |
| | 27 | 23 | 18 | 18 | 19 | 15 | 120 |

presenting no significant trend overall for the 2001–2012 period ($p = 0.07$) (Table 3). Still, croplands were the only land cover class, among the three main land cover classes in the watershed that was moderately and positively associated with the water surface reflectance at the three outlet sites (Table 4, shows the results of a confusion matrix evaluating the accuracy of the land cover classification. 67.5% was the overall accuracy. The most accurate land cover classification was urban with a 100% accuracy followed in order by water, wetland, forest, grassland and cropland with an 89.5%, 73.3%, 66.7%, 52.2% and 40.7%, respectively. It is important to mention that the land cover evaluation was conducted in December of 2014 and the MCD12Q1 product used was 2012.

## 5. Discussion

The low availability of data during the rainy seasons, appreciated from the Julian day axis on Fig. 3, is due to the fact that the MOD09GQ product registers surface reflectance in the red section of the spectrum (620–670 nm). Any radiation in the visible wavelength is obstructed by clouds, which are obviously more abundant during the rainy season.

Since we analyzed the inter-annual water surface reflectance temporal trends based solely on data from the first three months of the year, which are also the driest, the fluctuation of such trends do not necessarily represents the fluctuation of the inter-annual impacts on the Rosario Islands. However, even though the described cloud coverage issue impede trend analysis during the seasons where most sediment loading is expected, still temporal trends analysis during the dry season are useful as they show the conditions at which the impact is expected to be lower. Consequently, any influence occurring during the dry season (lower expectancy of impact) could be indicative of even stronger influence during the rainy season (higher expectancy of impact).

Similar principle would apply to spatial analysis. If such plumes get very close to the islands during periods where the sediments loads are the lowest, then they might be more likely to reach during the rainy season when the loadings are heavier. Figs. 5 and 6 show the spatial patterns of water surface reflectance during dry season according to which the plumes originated from Barbacoas Bay show to be the most likely to reach the Rosario Islands. Plumes from Cartagena Bay and Bocas de Ceniza are shown in the images of Figs. 5 and 6 to be in general not likely to reach Rosario Islands, although Figs. 5d, i and l and 6b show to reach close to the northernmost island of this archipelago even during the dry season. It is important to mention that during December–February the wind is blowing south-westward, which may favor the reach south of the sediments plumes but during the rest of the year it blows north-eastward along with the PCC (Mogollón-Vélez, 2013), making it less likely for sediment plumes from Bocas de Ceniza and Cartagena Bay but more likely for plumes from Barbacoas Bay to reach the islands.

The parallel inter-annual trends of water surface reflectance at Bocas de Ceniza, the bays of Cartagena and Barbacoas and the trend of rainfall on the watershed up to 2011 confirm the expected role of rainfall influencing water surface reflectance. 2011 and the second half of 2010 were years of one of the most intense La Niña events occurred during the last five decades (Hoyos et al., 2013). Due to the exceptionally high level and pressure of the Canal del Dique waters, on November 30 of 2010 occurred a breaking of the levee on the northern bank of the Canal del Dique (Correa, 2010). According to the media, this breaking discharged $10 \times 10^6$ m$^3$ of water before finally being repaired (Herrera-Delghams, 2011) flooding 500 km$^2$ of land with towns, cultivation and pastures for livestock (Correa, 2010). Fig. 9a–g, displays a sequence of MOD09GQ images covering the time period between dry land on October 13, 2010, until February 2, 2011, when still a small plume can be appreciated 64 days after the rupture. Since this period of time was located within the three months used here to calculate the inter-annual trend, it is possible that the diverted flow might have significantly reduced the outflow through Cartagena Bay and Barbacoas Bay. That would explain the lower surface reflectance recorded in 2011 for those sites during those three months as compared with values recorded in 2012 when the rainfall was lower. In fact, the values recorded at Bocas de Ceniza, as expected, were higher in 2011 as compared with those in 2012. Extra dredging activity in the Canal del Dique intensified after the breaking of the levee in November of 2010, including a major project signed on 2013 to control floods along the Canal del Dique (El Espectador, 2014) may explain the different behavior on the water surface reflectance trends at the bays of Cartagena and Barbacoas as compared with that of Bocas de Ceniza.

The absence of a trend line in the water surface reflectance at the Rosario Islands associated with those at the watershed outlets or with that of rainfall over the watershed (during the same inter-annual period using the same three months of each year) should not be interpreted as a lack of effect from the watershed in the water quality at the Rosario Islands but just as not enough sensitivity in our RS data to detect a possible relationship. Furthermore, the concentration of sediments in the water column required to adversely affect the health status of the coral can be much lower than that enough to be detected by RS. In fact, the spatial analysis of plumes from the outlets clearly detects an overlap on the islands surrounding waters with the plumes from Barbacoas Bay and in less magnitude with those from Cartagena Bay.

The discrepancy between having detected a significant inter-annual rainfall trend for the interval 2001–2013 when considering the entire year but not when using the first three months of each year for the period 2001–2014, can be explained by the fact that there is also a variability in intensity and duration of the rainy and dry bimodal seasons within the year from year to year. Therefore, a below-normal rainfall in a given trimester within the year for a given year does not translate into a below-normal rainfall for that year as compared with other years. Furthermore, a time period longer than that used in this study is needed to more accurately approximate conclusions about inter-annual trend lines for rainfall and water surface reflectance Fig. 10.

The apparent coincidence in the fluctuation patterns of the inter-annual trend lines of water surface reflectance and rainfall with a fluctuation of El Niño and La Niña (CPC, 2014), align well with a consistent ENSO-precipitation relationship reported in the literature for this study area, with below and above normal rainfall associated with El Niño and La Niña, respectively (Ropelewski and Halpert, 1987; Mason and Goddard, 2001; Restrepo and Kjerfve, 2000). However, the coincidence with water surface reflectance demands more research since to our knowledge it has not been reported before. Presumably, El Niño months presented lower water surface reflectance at the outlets due to the lower sediment loads caused in turn by the lower rainfall on the watershed. Conversely, the higher rainfall during La Niña years may have increased the transport of eroded material that cause increased water surface reflectance at the watershed outlets. The fluctuation in the rainfall pattern following the El Niño/La Niña events has been reported to be increasing in frequency (Cai et al., 2014). Therefore, a possible more frequent occurrence of La Niña years and associated higher rainfall and sediments discharges could translate into a growing adverse impact into the islands' corals.

Because cropland was the only land cover class directly associated with the water surface reflectance at the outlet sites (Table 4) and because such association could be plausible, it is tempting to suggest the land cover class as a critical human factor influencing water surface reflectance at the watershed outlets. Such

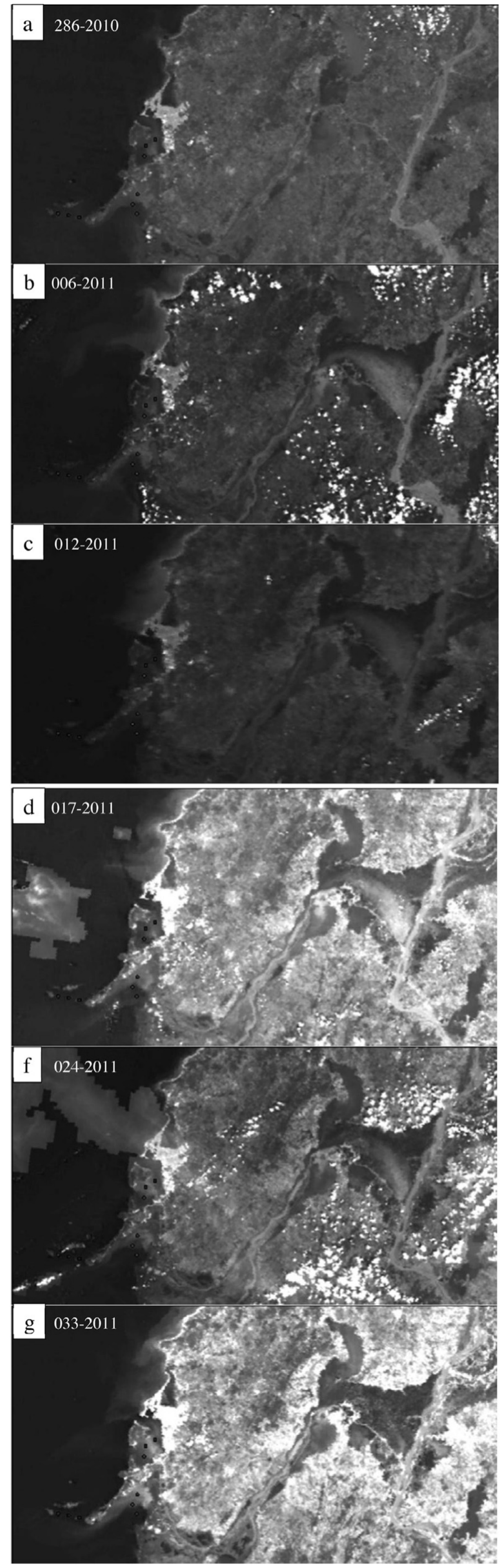


**Fig. 9.** Sequence of MOD09GQ (Band 1) images depicting the process of flooding. (a) October 13, 2010, land adjacent to Canal del Dique not yet flooded. The rupture of the embankment occurred on November 30, 2010, (b) January 6, 2011, shows a strong plume discharging into the flooded area. The entrance of water from the Canal del Dique into the disaster area continues although gradually decreasing in intensity as can be deduced from the fading plume shown on images of January (c) 12, (d) 17 and (e) 24 of 2011, and February 2 of same year.

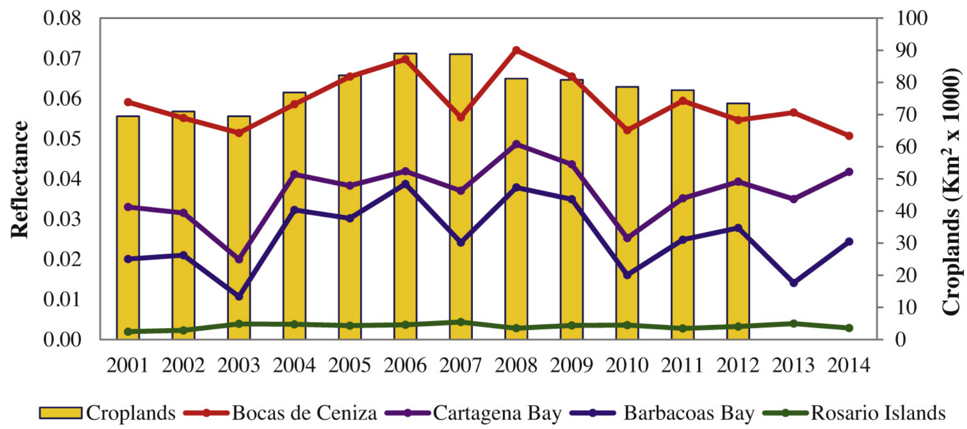


**Fig. 10.** In lines, 2001–2014 time series of inter-annual mean cloud free median surface reflectance (MOD09GQ) during the first 90 days of each year for the four sites monitored. In bars, 2001-2012 time series of MODIS estimated inter-annual trend of Croplands cover change.

relationship could be explained by the increased erosion and transport of sediments to outlet waters caused by agriculture (Moreno Madriñan et al., 2012). However, the low accuracy in the cropland classification of only 40.7% demands further analysis with a more reliable land cover classification product to draw confident conclusions.

## 6. Conclusions

Using the Magdalena River as a case study, we proved a successful application of the RS products MOD09GQ (for water surface reflectance) and TRMM 3B43V7 (for rainfall) to identify and monitor, temporally and spatially, the influence of regional rainfall and subsequent river discharges on the water surface reflectance at the outlets of a river with high fluxes and sediment loads. Although based on temporal trend line analysis alone it was no possible to statistically detect the influence on the water at the adjacent Rosario Islands in our case study, the visual inspection of satellite imagery let identify intrusion of sediment plumes into the islands waters, which suggests such influence, especially regarding plumes from Barbacoas Bay (Fig. 6). The coincidence noticed between La Niña conditions, above-normal rainfall on the watershed and above-normal water surface reflectance at the outlets merits research regarding potential effects of a possible climate change on the health of these coral reefs at the Rosario Islands.

A preliminary analysis based on MCD12Q1 data suggests agricultural land cover as the main land cover class influencing water surface reflectance at the watershed outlets. However, the low accuracy detected with the land cover validation demands further analysis with a more accurate land cover product. With the growing need to monitor and measure the effects of climate change and an increasing human activity on watersheds and coastal ecosystems both at the regional scale and at the world wide level, the products and procedures followed here can prove helpful for application on other coastal regions especially under conditions of scarcity or unavailability of *in situ* data. Such conditions are particularly common in developing countries where a large and growing proportion of the world's population is living in coastal areas.

## Acknowledgments

This research was conceived and initiated while the main author was working with SERVIR at the Marshall Space Flight Center (MSFC) during his fellowship with the NASA Postdoctoral Program (NPP). Partial funds were provided by SERVIR/MSFC through the NPP under contract with Oak Ridge Associated Universities. We thank Africa Flores-Cordova from University of Alabama in Huntsville (UAH) for her help with SRTM data and delineating the watershed and Dr. Ashutosh Limaye from NASA/MSFC for his advice with the use of TRMM data. We also thank Damien Jules Sulla-Menashe from Boston University for his advice regarding use and limitations of the land cover product, MCD12Q1.

## Appendix A. Supplementary data

Supplementary data associated with this article can be found, in the online version, at http://dx.doi.org/10.1016/j.jag.2015.01.008.

## References

Carricat-Ganivet, J.P., Merino, M., 2001. Growth responses of the reef-building coral *Montastraea annularis* along a gradient of continental influence in the southern Gulf of Mexico. Bull. Mar. Sci. 68 (1), 133–146 (14).

Cai, W., Borlace, S., Lengaigne, M., Van Rensch, P., Collins, M., Vecchi, G., Timmermann, A., Santoso, A., McPhaden, M.J., Wu, L., England, M.H., Wang, G., Guilyardi, E., Jin, F.F., 2014. Increasing frequency of extreme El Niño events due to greenhouse warming. Nat. Clim. Change 4, 111–116, http://dx.doi.org/10.1038/NCLIMATE2100.

Cendales, M.H., Zea, S., Díaz, J.M., 2002. Geomorfología y unidades ecológicas del complejo de arrecifes de las Islas del Rosario e Isla Barú (Mar Caribe, Colombia). Rev. Acad. Colomb. Cienc. 26 (101), 497–510, ISSN 03070-03908.

Chen, Z., Hu, C., Muller-Karger, F.E., 2007. Monitoring turbidity in Tampa Bay using MODIS/Aqua 250-m imagery. Remote Sens. Environ. 109, 207–220, http://dx.doi.org/10.1016/j.rse.2006.12.019.

Correa, M.V., 2010. En Atlántico ya se ve más agua que tierra. El Colombiano, December 19, 2010. http://www.elcolombiano.com/BancoConocimiento/E/en_atlantico_ya_se_ve_mas_agua_que_tierra/en_atlantico_ya_se_ve_mas_agua_que_tierra.asp (accessed 16.08.14.).

Cortés, J., Risk, M.J., 1985. A reef under siltation stress: Cahuita, Costa Rica. Bull. Mar. Sci. 36 (2), 339–356.

Climate Prediction Center (CPC), 2014. National Oceanic and Atmospheric Administration (NOAA)/National Weather Service/Climate Prediction Center (CPC) webpage, September 4, 2014. http://www.cpc.noaa.gov/products/analysis_monitoring/ensostuff/ensoyears.shtml (accessed 22.09.14.).

Díaz, J.M., Barrios, L.M., Cendales, J., Garzón-Ferreira, J., Geister, J., López-Victoria, M., Ospina, G.H., Parra, F., Pinzón, J., Vargas, B., Zapata, F.A., Zea, S., 2000. Areas Coralinas de Colombia. Serie de Publicaciones especiales, vol. 5. INVEMAR, Santa Marta.

Doxaran, D., Froidefond, J.M., Castaing, P., Babin, M., 2009. Dynamics of the turbidity maximum zone in a macrotidal estuary (the Gironde, France): observations from field and MODIS satellite data. Estuarine Coastal Shelf Sci. 81, 321–332, http://dx.doi.org/10.1016/j.ecss.2008.11.013.

El Espectador, 2014. Soluciones para el Canal del Dique, El Espectador, August 13, 2014. http://www.elespectador.com/noticias/medio-ambiente/soluciones-el-canal-del-dique-articulo-510277 (accessed 21.08.14.).

EOS Clearing House (ECHO), 2013. NASA's Earth Observing System Data and Information System (EOSDIS), Version 10.81.8 March 2013. http://reverb.echo.nasa.gov (accessed 30.05.14.).

Fabricius, K.E., De'ath, G., Humphrey, C., Zagorskis, I., Schaffelke, B., 2012. Intra-annual variation in turbidity in response to terrestrial runoff on near-shore coral reefs of the Great Barrier Reef. Estuarine Coastal Shelf Sci. 116, 57–65, http://dx.doi.org/10.1016/j.ecss.2012.03.010.

Friedl, M.A., Sulla-Menashe, D., Tan, B., Schneider, A., Ramankutty, N., Sibley, A., Huang, X., 2010. MODIS Collection 5 global land cover: Algorithm refinements and characterization of new datasets. Remote Sen. Environ. 114, 168–182.

Goddard Earth Sciences Data and Information Services Center (GES DISC), 2014. TRMM Online Visualization and Analysis System (TOVAS), Febrero, 27, 2014. http://disc.sci.gsfc.nasa.gov/precipitation/tovas (accessed 27.06.14.).

Herrera-Delghams, L., 2011. 57 días duró batalla contra boquete del Canal del Dique, El Tiempo, January 26, 2011. http://www.eltiempo.com/archivo/documento/MAM-4360599 (accessed 21.08.14.).

Hoyos, N., Escobar, J., Restrepo, J.C., Arango, A.M., Ortiz, J.C., 2013. Impact of the 2010–2011 La Niña phenomenon in Colombia, South America: the human toll of an extreme weather event. Appl. Geogr. 39, 16–25.

Hu, C., Chen, Z., Clayton, T.D., Swarzenski, P., Brock, J.C., Müller-Karger, F.E., 2004. Assessment of estuarine water-quality indicators using MODIS medium-resolution bands: initial results from Tampa Bay, Florida. Remote Sens. Environ. 93, 423–441.

IDEAM, 2001. Estudio ambiental de la Cuenca Magdalena-Cauca y elementos para su ordenamiento territorial. In: Technical Report and Arcinfo Database. Instituto de Hidrología, Metereología y Estudios Ambientales (IDEAM), Bogotá, Colombia, 984pp.

Land Processes Distributed Active Archive Center (LP DAAC), 2013. U.S. Geological Survey (USGS), Global Data Explorer website, September 6, 2013. http://gdex.cr.usgs.gov (accessed 20.06.14.).

Land Processes Distributed Active Archive Center (LP DAAC), 2014. U.S. Geological Survey (USGS)/Land Processes Distributed Active Archive Center (LP DAAC) webpage, April 14, 2014. https://lpdaac.usgs.gov/product/ (accessed 27.06.14.).

Libhaber, M., 2004. Establishing wastewater treatment levels in developing countries; stringent effluent standards versus absorption capacity of receiving bodies. The World Bank, The Latin American and Caribbean Region, presented in the Water Week, February 24–26, 2004. http://siteresources.worldbank.org/EXTWSS/Resources/337301-1147283808455/2532553-1149773755764/Libhaber_Presenation_in_Water_Week_2004_Short.pdf (accessed 07.01.15.).

Mason, S.J., Goddard, L., 2001. Probabilistic precipitation anomalies associated with ENSO. Bull. Am. Meteorol. Soc. 82, 619–638 http://dx.doi.org/10.1175/1520-0477(2001)082<0619:PPAAWE>2.3.CO;2

Miller, R.L., Liu, C., Buonassissi, C.J., Wu, A.-M., 2011. A multi-sensor approach to examining the distribution of total suspended matter (TSM) in the Albemarle-Pamlico estuarine system, NC, USA. Remote Sens. 3 (5), 962–974, http://dx.doi.org/10.3390/rs3050962.

Mobley, C.D., 1994. Light and Water: Radiative Transfer in Natural Waters. Academic Press, Inc., San Diego, CA, USA, pp. 60–144.

Mogollón-Vélez, J.V., 2013. El Canal Del Dique, El Áncora Editores, Bogotá, Colombia.

Moreno Madriñan, M.J., Al-Hamdan, M.Z., Rickman, D.L., Muller-Karger, F.E., 2010. Using the surface reflectance MODIS Terra product to estimate turbidity in Tampa Bay, Florida. Remote Sens. 2, 2713–2728, http://dx.doi.org/10.3390/rs2122713.

Moreno Madriñan, M.J., Al-Hamdan, M.Z., Rickman, D.L., Ye, J., 2012. Relationship between land cover/land use change and water turbidity of Tampa Bay major tributaries, Tampa Bay, Florida. Water Air Soil Pollut. 223, 2093–2109, http://dx.doi.org/10.1007/s11270-011-1007-2.

Morrison, J.M., Nowlin Jr., W.D., 1982. General distributions of water masses within the Eastern Caribbean Sea during the winter of 1972 and fall of 1973. J. Geophys. Res. 87 (6), 4207–4229, http://dx.doi.org/10.1029/JC087iC06p0420.

Petus, C., Chust, G., Gohin, F., Doxoran, D., Froidefond, J., Sagarminaga, Y., 2010. Estimating turbidity and total suspended matter in the Adour River plume (South Bay of Biscay) using MODIS 250-m imagery. Cont. Shelf Res. 30 (5), 379–392, http://dx.doi.org/10.1016/j.csr2009.12.007.

Pujos, M., Pagliardini, J.-L., Steer, R., Vernette, G., Weber, O., 1986. Influence of the north Colombian counter-current on the circulation of the continental platform: its action on the dispersion of effluents in suspension from the Magdalena River. Bull. Sci. Cent. Invest. Oceanogr. Hydrogr. 6, 3–15.

Restrepo, J.D., Kjerfve, B., 2000. Magdalena River: interannual variability (1975–1995) and revised water and sediment load estimates. J. Hydrol. 235 (1–2), 137–149, http://dx.doi.org/10.1016/S0022-1694.

Restrepo, J.D., Kjerfve, B., 2002. River discharge, sediment load, and sediment yield estimates for the Magdalena River and other Caribbean rivers of Colombia: environmental implications. In: Kjerfve, B., Kremer, H., Salomons, W., Crossland, J.M. (Eds.), CariBas – Activities in River Catchments and their Impacts on Coastal Systems in the Caribbean, LOICZ-IGBP Report, No. 23.

Restrepo, J.D., Kjerfve, B., 2004. Hydrochemical aspects of major Pacific and Caribbean rivers of Colombia. In: Lacerda, L.D., Santelli, R.E., Duursma, E., Abrao, J.J. (Eds.), Facets of Environmental Geochemistry in Tropical and Subtropical Environments. Springer Verlag, Berlin, pp. 169–187.

Restrepo, J.D., Lopez, S.A., 2007. The environmental database of Colombian deltas with emphasis on the Magdalena River. Dynamics and Vulnerability of River Delta Systems, A Scoping Workshop CDMS INSTAAR, Boulder, Colorado, USA, September 2007. http://csdms.colorado.edu/w/images/Juan_wednesday_afternoonMagdalena.ppt.pdf (accessed 07.01.15.).

Restrepo, J.D., Kjerfve, B., Hermelin, M., Restrepo, J.C., 2006a. Factors controlling sediment yield in a major South American drainage basin: the Magdalena river, Colombia. J. Hydrol. 316, 213–232, http://dx.doi.org/10.1016/j.jhydrol.2005.05.002.

Restrepo, J.D., Zapata, P., Díaz, J.M., Garzón-Ferreira, J., García, C.B., 2006b. Fluvial fluxes into the Caribbean Sea and their impact on coastal ecosystems: the Magdalena River, Colombia. Global Planet. Change 50, 33–49, http://dx.doi.org/10.1016/j.gloplacha.2005.09.002.

Rodríguez-Guzmán, V., Gilbes-Santaella, F., 2009. Using MODIS 250 m imagery to estimate total suspended sediment in a tropical open bay. Int. J. Syst. Appl. Eng. Dev. 1 (3), 36–44.

Ropelewski, C.F., Halpert, M.S., 1987. Global and regional scales precipitation associated with El Nin˜o-southern oscillation. Mon. Weather Rev. 115, 1606–1626 http://dx.doi.org/10.1175/1520-0493(1987)115<1606:GARSPP>2.0.CO;2

Sánchez, J.A., 1995. Benthic communities and geomorphology of the Tesoro Island reef, Colombian Caribbean. An. Inst. Invest. Mar. Punta Betín 24, 55–77.

Sánchez, J.A., Alvarado, E.M., Gil, M.F., Charry, H., Arenas, O.L., Chasqui, L.H., García, R.P., 1999. Synchonous mass spawning of *Montastraea annularis* (Ellis & Solander) (Faviidae: Scleractinia) at Rosario Islands, Caribbean Coast of Colombia. Bull. Mar. Sci. 65 (3), 873–879.

West, K., Woesik, R.V., 2001. Spatial and temporal variance of river discharge on Okinawa (Japan): inferring the temporal impact on adjacent coral reefs. Mar. Pollut. Bull. 42 (10), 864–872, http://dx.doi.org/10.1016/S0025-326X(01)00040-6.

Wust, G., 1963. On the stratification and the circulation in the cold water sphere of the Antillean-Caribbean basin. Deep Sea Res. 10, 165–187.